Applied Physics A (2021) 127:622
https://doi.org/10.1007/s00339-021-04770-9

Applied Physics A
Materials Science & Processing

Common issues in the hetero-epitaxial seeding on SiC substrates in the sublimation growth of AlN crystals

R. Radhakrishnan Sumathi[1]

Received: 11 January 2021 / Accepted: 14 July 2021 / Published online: 24 July 2021

Abstract
Aluminium nitride (AlN) is a futuristic material for efficient next-generation high-power electronic and optoelectronic applications. Sublimation growth of AlN single crystals with hetero-epitaxial approach using silicon carbide substrates is one of the two prominent approaches emerged, since the pioneering crystal growth work from 1970s. Many groups working on this hetero-epitaxial seeding have abandoned AlN growth altogether due to lot of persistently encountered problems. In this article, we focus on most of the common problems encountered in this process such as macro- and micro-hole defects, cracks, 3D-nucleation, high dislocation density, and incorporation of unintentional impurity elements due to chemical decomposition of the substrate at very high temperatures. Possible ways to successfully solve some of these issues have been discussed. Other few remaining challenges, namely low-angle grain boundaries and deep UV optical absorption, are also presented in the later part of this work. Particular attention has been devoted in this work on the coloration of the crystals with respect to chemical composition. Wet chemical etching gives etch pit density (EPD) values in the order of 10^5 cm^{-2} for yellow-coloured samples, while greenish coloration deteriorates the structural properties with EPD values of at least one order more.

Keywords Semiconductor materials · Aluminium nitride · Hetero-epitaxy · Crystal coloration · SiC substrates · Deep UV · High-power devices

1 Introduction

Wurtzite aluminium nitride (AlN) is a semiconductor material, important for the development of ultraviolet (UV) light sources and UV photodetectors, and for using as a buffer layer or a native substrate for nitride-based electronic devices due to its wide band gap (6.089 eV at low temperatures) [1]. Appliance of these devices, for example, as high-efficiency small and compact deep UV light-emitting diodes (LEDs) and laser diodes (LDs) for reinstating the low-efficiency and highly toxic mercury lamps and gas lasers used in water/air purification and disinfection or for high-resolution photolithography is based on AlN and high-aluminium (Al)-content aluminium gallium nitride (AlGaN). Enabling such far-reaching applications with a realization of eco-friendly technology based on AlN and their alloys is an immense benefit and is a must. For nontoxic solid-state lighting applications, the potentials of low-dimensional materials like quantum dots, nanocrystals have additionally attracted extensive attention [2, 3]. The results of UV LEDs based on AlN or AlGaN quantum dots have also been published by other groups [4, 5]. It was shown that the performance of AlGaN-based UV LEDs could be increased, especially due to the improved quality of AlGaN layers with high Al content [6]. The efficiency might further be increased using AlN single crystalline wafer as a substrate, since epitaxial AlGaN layers grown on such lattice-matched substrates by metalorganic chemical vapour deposition (MOCVD) method have significantly lower dislocation densities.

Crack-free AlGaN layers up to 2 µm thickness were grown on sapphire substrates by hydride vapour phase epitaxy (HVPE), and also 40-µm-thick crack-free AlGaN layers on SiC substrates were reported [7]. For high-Al-content $Al_xGa_{1-x}N$ (x ~ 0.7–0.8) layers grown on sapphire, high-resolution X-ray diffraction rocking curve (XRD-RC) widths ranging from 250 to 650 arcsec and from 1400 to 1900 arcsec were reported for the (00.2) symmetric and (10.2) asymmetric reflections, respectively. These layers contain high

✉ R. Radhakrishnan Sumathi
sumathi@lrz.uni-muenchen.de

[1] Applied Crystallography and Materials Science Institute, Ludwig-Maximilians-University (LMU), D-80333 Munich, Germany

densities of screw dislocations (6 x 10^8 cm^{-2}) and edge dislocations (2 x 10^9 cm^{-2}). Similarly, $Al_xGa_{1-x}N$ (x = 0.54) films grown on sapphire substrate by low-pressure MOCVD have also been reported [8], and the films exhibited the (00.2) XRD-RC full width at half maximum (FWHM) of about 597 arcsec. It has also been reported that a thick $Al_xGa_{1-x}N$ (with x = 0.6) layers on low-defect-density bulk AlN substrates could be achieved [9] with a thickness far exceeding the critical thickness as given by the Matthews and Blakeslee model. Furthermore, these grown layers with this composition were pseudomorphic. This work demonstrates the use of low-defect-density material for high-power UV LEDs. The use of low-defect-density bulk AlN substrates was shown to lead reliable UV LEDs capable of mW level power outputs that are emitting from 250–275 nm [10]. Because of this, there is a great push for the progress in the growth of high-quality bulk AlN crystals as substrates for deep UV LEDs.

Crystal quality, in terms of defects and impurities in AlN, affects device performance, and it is important to understand their properties and engineering them for realizing substrates with low dislocation density and transparency in the UV-C region. Like another III-N material family—gallium nitride (GaN), the availability of AlN substrates in terms of both size and quality (till now only up to 2 inch diameter) is still rather limited and very expensive as compared to conventional III-V materials, namely gallium arsenide (GaAs) and indium phosphide (InP) substrates (available even up to 4 inches dia.). So far, sublimation–recondensation growth, so-called physical vapour transport (PVT) growth, of bulk AlN either by homo-epitaxy after native seeding on self-nucleated crystals and subsequent crystal diameter enlargement with repeated growth process or by hetero-epitaxial seeding on selective substrates like silicon carbide (SiC) are reported widely and are more successful. Homo-epitaxial growth realizes a much higher crystalline quality with a lower dislocation density but enlarging the AlN crystals to a size suitable for industrial scale ($\geq$ 4 inch) remains a challenge. One of the advantages of the latter method is the commercial availability of large diameter (up to 6 inches) SiC wafers. In particular, the preparation of single crystalline AlN substrates by this approach is attractive if a large diameter substrate production is necessary and one wishes to bring down the wafer cost. However, structural quality of the SiC substrate is crucial, and high-quality wafers with less micro-pipe defect density are required to minimize the decomposition of the SiC substrate and to reduce defects in the grown AlN. A full UV transparency of this AlN material remains an open issue due to the observation of optical absorption typically in the blue and UV range due to chemical impurities.

Scrutinization of nearly all PVT-grown AlN crystals exhibits a coloration (yellow or dark amber or even dark green colour) due to the presence of chemical impurities and point defects. The impurity incorporation and point defect creation are relatively easy in such a high-temperature growth process. All these are expected to introduce defect/impurity related energy states in the band gap of the material and may cause light absorption at the sub-band gap that can interfere with the operation of optoelectronic devices. Impurity identification studies show that most common impurities are unintentionally incorporated in the grown material and may be having a greater role on the sudden drop of transmission curve at the energies lower than the band gap [11]. In Table 1, the onset absorption edge energy values of different coloured AlN samples are presented [12–15]. Oxygen (O) was regarded as the main impurity that contaminates the AlN crystals, and it was noticed that the incorporation of oxygen is accompanied by the formation of Al vacancies (V_{Al}). Also, it has been suggested that complexes of Al vacancies and oxygen on a nitrogen (N) site are the dominant form of V_{Al} in as-grown AlN samples with the use of positron annihilation studies (PAS). Furthermore, defects on the nitrogen sub-lattice (either O_N or V_N) have been observed by electron paramagnetic resonance (EPR) examinations [16]. Based on these various experimental observation results, preliminary assignments and possible explanations on the microscopic mechanisms have been given. Further progress to infer more detailed information and to get a complete picture about these states in AlN is needed, especially on those optical absorptions including the deep levels which possibly affect the performance of devices.

The PVT growth of AlN on SiC was intensively endeavoured by many research groups in the last decade. But, because of various issues faced with, this approach has not been considered as a prominent one by many researchers, and they have not continued working with this approach

Table 1 Absorption edge and etch pit density (EPD) values of different coloured AlN crystals

Crystal colour	Absorption edge	EPD	References
Transparent (colourless)	5.1 eV	2 x 10^5 cm^{-2}	Wang et al. 2019 [12]
Yellow	4.4 eV	4 x 10^5 cm^{-2}	Bickermann et al. 2012 [13], Sumathi et al. 2013 [14]
Amber	4.3 eV	6 x 10^5 cm^{-2}	Sumathi et al. 2013 [14], Tandon 2009 [15]
Green	4.0 eV	1.6 x 10^6 cm^{-2}	Bickermann et al. 2012 [13], Tandon 2009 [15]
Dark green	3.7 eV	NA	Bickermann et al. 2012 [13]

[17–20]. Nevertheless, a very few research groups like us have given serious consideration to this approach and kept continued working on this hetero-epitaxial growth method [21–24]. To give an illustration of one such problem, the observation of broad peaks in the blue and UV region of the AlN absorption spectra is a big concern for the material grown with the PVT system. On the other hand, this problem is not only specific to PVT, but also, as it was later found that the material synthesized by other methods like MOCVD [25], NH_3 source molecular beam epitaxy (MBE) has also shown up such phenomenon. In this contribution, we present and discuss in detail the common issues of the hetero-epitaxial growth of AlN material on SiC substrate. Particular attention was devoted to the frequent problems encountered during bulk crystal growth, and their underlying process-controlled solutions were investigated to solve some of the issues, if not all.

2 Experimental details

AlN single crystals were hetero-epitaxially grown on Si-face, (0001) SiC substrates by the PVT method using an inductively heated reactor. Hexagonal polytypes (6H and 4H) of SiC substrates were used with different off-orientations (0°, 2° and 4°—off from (0001) plane towards [110] direction). Bulk crystal growth was performed at the temperature range of 1800–1900 °C in tantalum carbide (TaC) crucibles under nitrogen (N_2) atmosphere. Almost all the grown crystals, investigated in this study, were of about 20–28 mm in diameter and up to 7 mm in thickness. AlN source powder has been sintered at high temperatures of around 2000°C for purification. The sintered source contains reduced oxygen (0.02 wt%) and carbon (0.01 wt %) impurities as measured by glow discharge mass spectrometry (GDMS). Our crystal growth process of AlN can be outlined as follows: (1) sublimation of sintered solid AlN source material kept at the bottom of a TaC crucible, (2) mass transport of the sublimed gaseous Al and N_2 species driven by high thermal gradients and (3) deposition of crystalline AlN material on the SiC substrate (placed on the crucible top) by recondensation of the vapour. The desired high-temperature gradient along the crucible was accomplished by moving the position of the inductive coil relative to the crucible. This is important for having a significant aluminium (Al) partial pressure and to increase the reactivity of N_2, so that reasonable growth rates are attained. By taking into consideration the etching of the substrate by vigorous Al vapour, a moderate growth rate of 20–40 µm/h has been achieved. The growth rate can further be increased through a careful increment in the axial temperature gradient in the system, without accelerating the decomposition and/or etching of SiC substrate by Al vapour at high growth temperatures and also not affecting growth mode. In this PVT configuration, the source, vapour, seed and the growing crystal are contained within the crucible. So, the impurity content of the grown crystals mainly depends on the source purity as well as the crucible material that should be properly selected.

In order to assess the structural quality (mosaicity) of the grown crystals, high-resolution X-ray diffraction (HRXRD) measurements were taken using Phillips X'pert Epitaxy diffractometer, in double axis geometry with a four bounce Ge[220] monochromator for Cu $K_{\alpha 1}$ radiation, which provides an intense and highly collimated beam. An open detector (minimum step 0.0001°) was utilized to obtain the rocking curves (RC). RCs of symmetric 0002 reflection were obtained from the as-grown surface of the samples. The X-ray beam footprint on the measured samples was approximately 1 x 2 mm^2. Surface morphology of the crystals was examined by optical as well as laser scanning microscopy (LSM). Chemical analyses were carried out using electron probe microanalysis (EPMA) and X-ray photoelectron spectroscopy (XPS) techniques. CAMECA SX100 EPMA apparatus with 5 spectrometers was used in the wavelength-dispersive spectroscopy (WDS) mode for the simultaneous measurements of all the expected elements (Si, Al, C and N) from AlN grown on SiC. K_α lines of these elements measured separately with different spectrometers were analysed for obtaining the quantitative information of their incorporation into the grown crystals. Nominally pure AlN crystal and highly pure commercial SiC crystal samples were used as standard references for the calibration. Surfaces of both the standards and the measurement samples were coated with 15 nm carbon layer for better conductivity to avoid surface charging. In addition to (0001) surfaces, cross-sectional samples were also prepared to investigate the incorporation of Si and C along the grown crystal length by EPMA. The XPS measurements were taken using a PHI 5000 VersaProbe II with a focused and monochromatic X-ray source (Al-Kα, 1486.68 eV), at approximately 12 kV and a vacuum of 10^{-9} mbar. The detected binding energy range was from 0 to 600 eV. Further analyses on impurities were performed by Fourier transform infrared (FTIR) spectroscopy measurements. For this, an Equinox 55 FTIR spectroscope (Brucker) was used. Defect-selective chemical etching was carried out using a KOH–NaOH (1:1) molten eutectic etchant, and the defect densities were estimated using both optical and LSM analysis. The surface finishing for most of the measurements was done with mechanical polishing using diamond paste up to the particle size of 0.25 µm, which resulted in the RMS surface roughness of around 4 nm, while chemo-mechanical polishing (CMP) was performed for the defect-selective etching studies.

3 Results and discussion: Various issues in Hetero-epitaxial growth

In hetero-epitaxial growth of crystalline material, the substrate plays a dominant role on the quality and the properties of the growing crystals such as dislocation density, surface morphology and some extent to chemical composition that is influenced by the impurity content. AlN layer grown on sapphire substrate by HVPE method shows high number of dislocations exhibited by the broad XRD rocking curves [26]. Further, AlN layers grown on Si (111) substrates exhibit the dislocation densities in the order of 10^8 cm^{-2} [27]. Hence, the choice of best substrate material is very compelling. Some of the prerequisites that should be considered, for choosing a substrate could be (1) good matching of lattice parameter, (2) close matching values of thermal expansion coefficient, (3) high structural perfection, (4) availability in large areas, (5) good thermal/chemical compatibility and (6) free supply at a reasonable cost. The thermal and chemical stabilities are additional specific criterion for this high-temperature AlN growth process. Both AlN and hexagonal SiC have the same space group of "$P6_3mc$". AlN has the "*a*" lattice constant value of 3.1106 Å, and for 6H SiC and 4H SiC, the "a" lattice constant values are 3.0805 Å and 3.0730 Å, respectively. So, the in-plane lattice constant mismatch of SiC with AlN is small, only about 1% (0.96% to 6H SiC and 1.2% to 4H SiC). In the light of the above-mentioned properties, 6H and 4H SiC substrates could fulfil the needed requirements and are the best possible candidates for the hetero-epitaxial seeding of AlN in the PVT growth. In particular, the thermal stability of SiC is moderately good at temperatures next to the lower limit of AlN crystal growth process. Nevertheless, there have been many scientific and technological challenges in this growth process to overcome, and we present and discuss here some of the major issues encountered in such crystal growth experiments.

3.1 Formation of hole defects in the crystals

When an AlN crystal is growing on SiC at high temperatures of around 1900 °C, decomposition at the backside of the SiC substrate could occur simultaneously, although the back surface is covered by a seed holder. Subsequently, this undesirable evaporation affects the growth process and could provoke the formation of micro-holes in AlN. The decomposition at the defect sites of the wafer is much faster than in a defect-free region. In addition, the micro-pipes inherently present in the SiC substrate follow through the growth direction of the crystals and affect the epitaxial growth. Micro-pipes are the crystallographic defects often found in SiC crystals that are created due to internal and external stresses during crystal growth [28]. They mostly arise due to the propagation of screw dislocations having larger Burgers vectors [29]. These micro-pipes present in the SiC substrate can replicate into overgrowing AlN layers and so could very well present in the AlN crystals too. Nonetheless, it is possible to overgrow these micro-pipes, if they were to emit dislocations into the adjoining matrix [30], together with the optimized and quick coverage of AlN during initial growth stages. It is well known that the SiC single crystals are grown at very high temperatures (>2000 °C) by the PVT technique and hence the stress management is very difficult. The commercially available 100-mm-diameter SiC wafers generally contain a micro-pipe density of around 10 up to a few hundred per cm^2. It is to be mentioned that the substrates used in this investigation contain nominal micro-pipe density, especially the 4H polytype. Once these micro-pipes start to propagate into the growing AlN crystal, then the crystal will contain several micro-holes of varying sizes (up to ~100 µm). Even macro-holes of 200 µm in size, as shown in Fig. 1b may also be formed due to strong back evaporation of AlN at this defect site. These holes are prominent in thin AlN crystals grown with less than 2 mm thickness, but only very few numbers are present over the whole surface of a crystal of 28 mm dia. The thin crystals (less than 2 mm thick) were usually grown with low growth rate, and hence, in this case, AlN layer could not quickly cover the SiC substrate, and also not thick enough to compensate the back evaporation. But, when the growth is performed with higher growth rates (to obtain bulk crystals of useful thickness), the surface of SiC is fastly covered by AlN layer in the initial stages itself and also thick enough to compensate the back evaporation at the micro-pipes and other defect sites. LSM height profile measurements were taken on the holes, shown in Fig. 1a, on the AlN crystal of approximately 500 µm thickness. As could be seen from LSM height profile (Fig. 1c), these holes are deeper than 600 µm, which is higher than the thickness of the actual AlN layer. It shows that the holes originate from the SiC substrate.

It is to be considered that two competing processes, namely growth of AlN and decomposition of SiC substrate, occur at the same time. If the AlN layer does not fully cover the SiC substrate before the strong decomposition starts, it will lead to the formation of such holes. This will be crucial for further usefulness of these grown AlN crystals, such as for native seeding for bulk growth or in epitaxial device fabrication. These holes could be reduced by covering the SiC substrate by AlN layer very quickly in the initial stages of the growth. Currently, SiC wafers with zero micro-pipe are sparsely available, and if they are used for this hetero-epitaxial growth of AlN under controlled growth conditions,

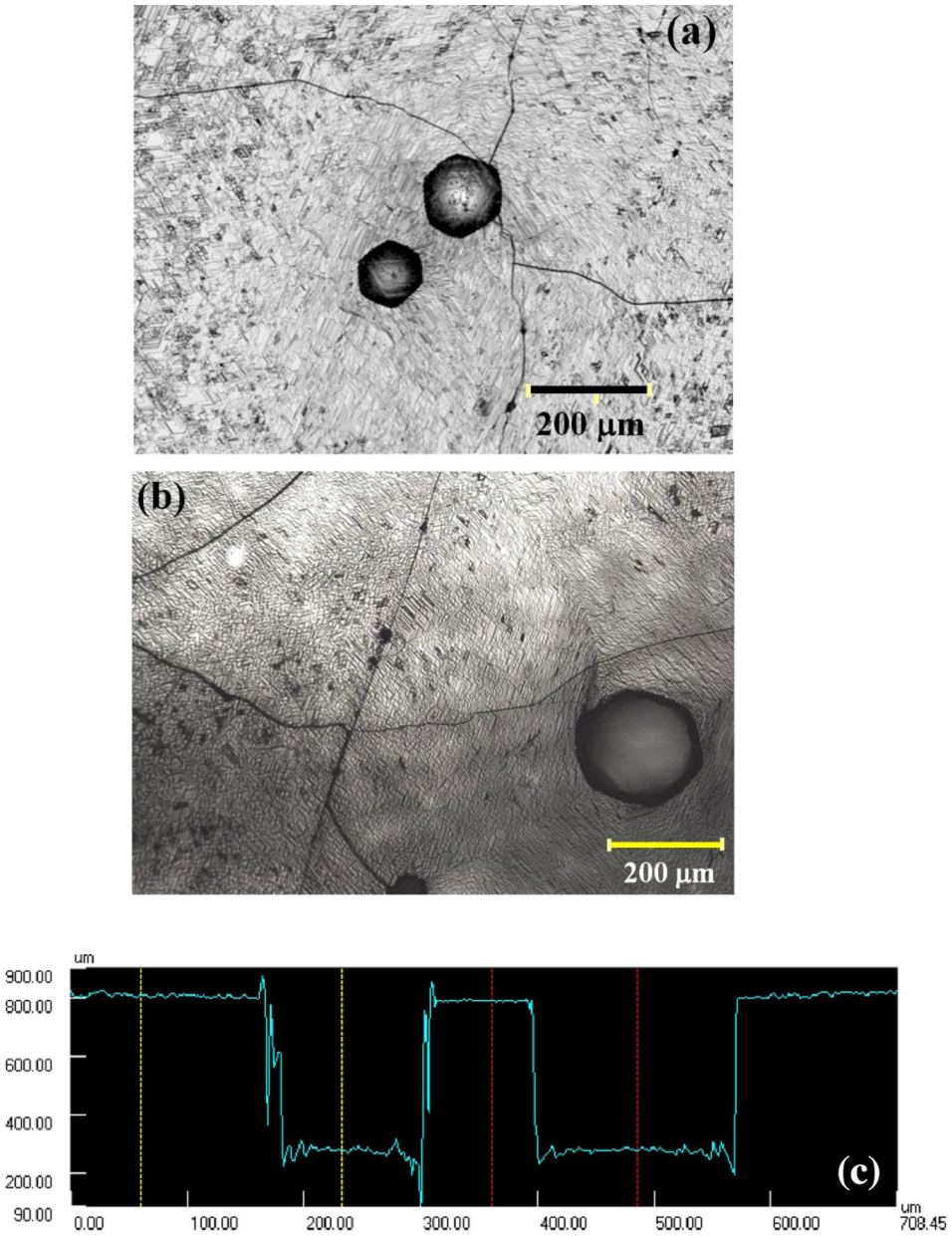

Fig. 1 **a**, **b** Laser scanning microscopy pictures of the as-grown surface of an AlN single crystal grown on SiC substrate, exhibiting hexagonally shaped macro-hole defect of more than hundred µm size, **c** LSM height profile of the micro-holes (in Fig.1a); the profile line starts from the left side hole and to the right side

then the formation of such micro-holes in AlN could further be minimized or eliminated.

3.2 Coloration of the crystals

As already described in "Experimental details" section, crucible plays a decisive role on the whole growth process. TaC crucibles are preferred rather than tungsten (W) crucibles for this hetero-epitaxial growth, because Si in SiC reacts with W and forms low-temperature eutectics such as tungsten silicides [31]. However, the utilization of TaC crucibles and SiC seeds in a graphite heater environment is naturally accompanied by the diffusion of Si and C into the growing AlN crystal. Such impurities, even in modest concentrations, can increase the point defect density of the crystal, change the crystal habit or account for absorption of visible wavelengths by AlN, thereby changing the colour of the crystals. The AlN crystals are usually transparent or light yellowish in colour, and in general, oxygen is considered to be the main impurity which causes the yellow colouration [11]. The presence of oxygen in the growth environment is detrimental because of the oxynitride and stacking faults formation [32], which can decrease the thermal conductivity and further may be the reason for specific below-band-gap absorption. Hence, that is also considered as a critical impurity which should be significantly reduced. Aluminium has a strong oxidation nature and the oxidized AlN source powder acts as a prime source for supplying oxygen to the vapour

phase during crystal growth. Even after sintering the source material at high temperatures (2000 °C) for several hours, before performing the growth experiment, the concentration of oxygen in the source may only be reduced to 0.02 wt%. In our crystals, we have observed both the yellow and green coloration as shown in Fig. 2a. The photograph of the cross-sectional sample cut from one such crystal is also given in Fig. 2b for clear perception. The upward arrow in the picture indicates the growth direction of the crystal (*c*-direction). It could be seen that the first 3–4 mm of the crystal (starting from the SiC substrate at the bottom) is yellowish and the top part with approximately 2 mm thickness is dark greenish in colour. This type of green coloration is often reported [13] in the literature as well. Some researchers even reported the deep blue colouration of AlN crystals [33]. In order to understand the cause of the green coloration, various investigations such as EPMA and XPS analyses have been performed. The EPMA results indicated that these coloured parts of the crystals have the average value of 2–4 at% Si and 5–8 at% C impurities, but fairly good regions of the crystals with yellow coloration have less impurity concentrations, of about 1.5–2 at% silicon and –5 at% carbon impurities. From our cross-sectional EPMA measurement results, we have seen that the Si concentration of approximately 10 at% is present very close to the interface, but this Si concentration greatly reduces to 2 at%, within a distance of 500 μm from the interface. A continuous decrease in the nitrogen content along the growth length of the crystal (blue arrow indicated in Fig. 2b) has also been evaluated from the EPMA measurement. It is known that the solubility of carbon is good in III-nitride compounds. With the assumption of the preferred incorporation of carbon on the nitrogen site, it can potentially be reasoned that the increasing carbon content in the crystal causes the dark green coloration in the top part of the crystal. Further confirmations have been made by FTIR spectroscopy measurements. A phonon mode related to the stretching vibration of carbon atoms (C=C) was identified in the FTIR spectrum (not shown here) at around 1650 cm^{-1}, only for the top part of the crystal where the strong coloration is seen. Hence, it is becoming more evident that the incorporation of unintentional carbon substitutes the N site. Carbon is an amphoteric impurity due to the fact that it is a group IV atom, and it behaves like a donor when it is incorporated on the cation site and like an acceptor if it is on the anion site. But, due to the wide band gap of AlN, it self-compensates itself and also creates a deep energy states, thereby acting as a trap for other charge carriers.

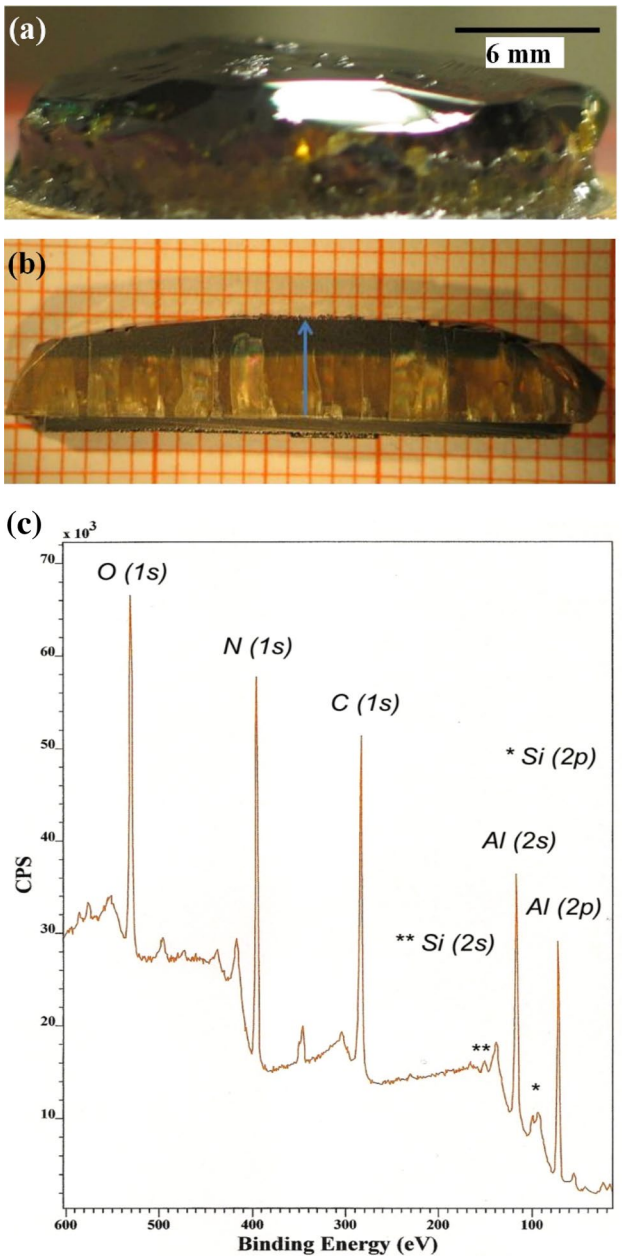

Fig. 2 **a** AlN single crystal grown on SiC substrate, showing both the yellow and green colouration; **b** interface cross section of one such AlN crystal grown on SiC; the arrow indicates the growth direction. The colour variation from yellow to green is clearly visible; **c** XPS spectra of a sample prepared from such a crystal showing silicon and carbon impurities. The binding energy was detected in the range from 0 to 600 eV

Another interesting observation made in our growth experiments is that when more carbon impurity is incorporated (i.e. in homo-epitaxy where there is no silicon environment), the crystals look to have brown coloration. But, if both silicon and carbon are incorporated in relative proportion, then the AlN crystal colour turns to be green. A SiC substrate with a high micro-pipe density may give up more volatile silicon and carbon in the vapour phase. In order to be convinced that the Si and C impurities are coming from the substrate (for C, additionally from crucible/heater environment) and not from the source material, the sintered AlN source powder has been analysed by X-ray powder diffraction measurements and subsequent Rietveld refinement

has been carried out. The refinement analysis shows only α-AlN phase, and no unintentional impurity phases could be detected in the sintered source powder. We have also performed EPMA measurements, but silicon and carbon could not be found out, because of the concentration under the detection limit. From our experimental investigations, we propose that different impurity environments and their incorporation during the growth process results in different coloration of the crystals; namely, (i) brown coloration is mainly due to carbon (even the crystals by homo-epitaxy in TaC crucible with graphite heater), (ii) green coloration is related to more silicon and carbon (mainly, crystals from hetero-epitaxy in TaC crucible and graphite environment), (iii) golden yellow coloration is primarily due to oxygen together with silicon and carbon (usually, minimized impurity incorporation in crystals from hetero-epitaxy in TaC crucible and graphite heater), and (iv) light yellow or transparent is mainly because of oxygen (homo-epitaxy crystal grown in tungsten crucible/heater set-up, in the absence of both silicon and carbon).

In the EPMA measurements, to avoid the surface charging effects, the surface of the sample was coated with a conducting carbon layer, and hence, the C concentration estimation may not be accurate. Moreover, detecting the light elements like carbon is very difficult in this EPMA technique. Hence, XPS measurements were taken to complement the EPMA measurements made on the good part of the crystals. XPS spectrum of the hetero-epitaxially grown AlN sample (yellow-coloured) is shown in Fig. 2c. The spectrum shows all the expected elements (Al, N, C, Si and O) from the AlN crystal grown on SiC. One can see that even in the yellow-coloured crystals/regions, silicon and carbon peaks with significant intensities are observed. The appearance of C-1s peak at 285 eV with higher intensity indicates high concentration of carbon incorporation, which correlates with our results of EPMA. This might be because of three different sources for carbon (substrate—SiC, crucible—TaC, heating element—graphite). Although the oxygen concentration of the sintered source material is around 0.02 wt%, surface of the AlN sample exhibits high-intensity XPS peak for oxygen and it may be due to native oxide formation on the surface after keeping the sample in the atmosphere for long time. Moreover, the sample was not sputtered with Ar-ion before taking the measurements. For silicon, both the Si 2p at around 101 eV and Si 2s at around 150 eV were detected, which matches well with the reported binding energy values in the literature [34]. The concentration of silicon impurity, quantitatively derived from Si 2p peak, is about 1.7 at%, and this value well correlates with the EPMA measurement data for Si. So, it can be inferred that even good quality, yellow-coloured AlN single crystals are being contaminated by certain amount of silicon from the substrate. The peak for Al appears for the electron configuration 2s at around 120 eV and 2p at around 75 eV. Nitrogen could be detected as 1s electron configuration with a peak at approximately 395 eV.

3.3 Crack formation in the crystals and polycrystalline rim

Different thermal expansion coefficients between AlN, SiC substrate (mismatch ~ 1%) and also TaC seed holder cause AlN crystal to become more stressed when it is cooled down to room temperature, after the completion of the growth process. Hence, the total thermal mismatch between these three materials is the reason for crack formation in the grown AlN crystal. As an example, the photograph of one of the 2-mm-thick AlN crystals is shown in Fig. 3a, and the cracks are

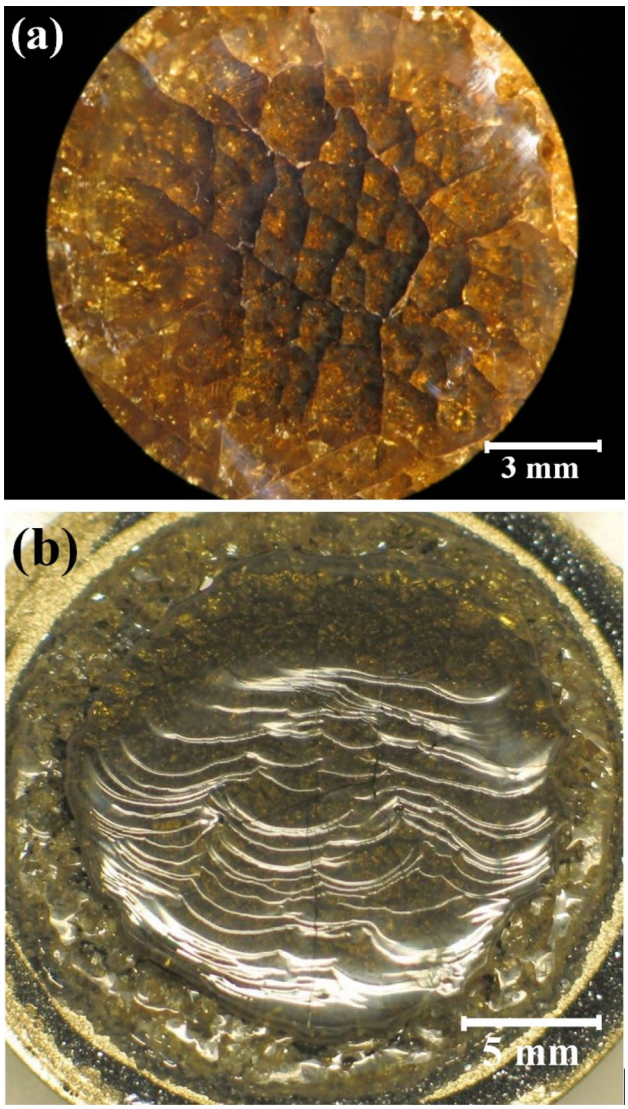

Fig. 3 Photographs of AlN single crystals. **a** Surface of a crystal exhibiting crack formation; **b** polycrystalline rim grown on TaC holder, surrounding the single crystalline part the crystal.

clearly seen on the surface of the crystal. The density of cracks increases when the single crystalline part is in contact with the surrounding AlN polycrystalline rim. The formation of AlN polycrystalline rim may be due to the fast evaporation of the SiC substrate peripheries/edges, wherein the substrate is rapidly and fully decomposing. Consequently, the crystal growth occurs on polycrystalline TaC seed holder in the edges, and hence, the polycrystalline AlN rim is formed (Fig. 3b) surrounding the single crystalline area. As AlN possesses anisotropic thermal expansion, it is understandable that the contact of the single crystal part with that of AlN poly rim will produce additional cracks in the single crystal. It leads to the problems in producing large-size AlN wafers for device processing and hence the cracks should be avoided. In homo-epitaxial growth, it is conventional that additional heating elements are inserted near the seed holder's edge to avoid such polycrystalline rim formation, but this may not be applicable in this case of hetero-epitaxial growth, since this will enhance the decomposition of SiC even faster.

3.4 Multi-source nucleation and high mosaicity

When on-axis (0° off-oriented) substrates are used for the growth experiments, 3D multi-source nucleation has been observed in the crystals even in the as-grown surfaces, as shown in Fig. 4a. The absence of steps and kink positions in these types of substrates leads to nucleation of grains (3D islands formation) at many different places of the surface of the seed, which might have started as 2D nuclei in the initial stages. Growth on an on-axis substrate offers large, atomically smooth surfaces and implies the presence of a kinetic barrier for adatoms and suppresses the diffusion length of adatoms. Hence, the layer coverage

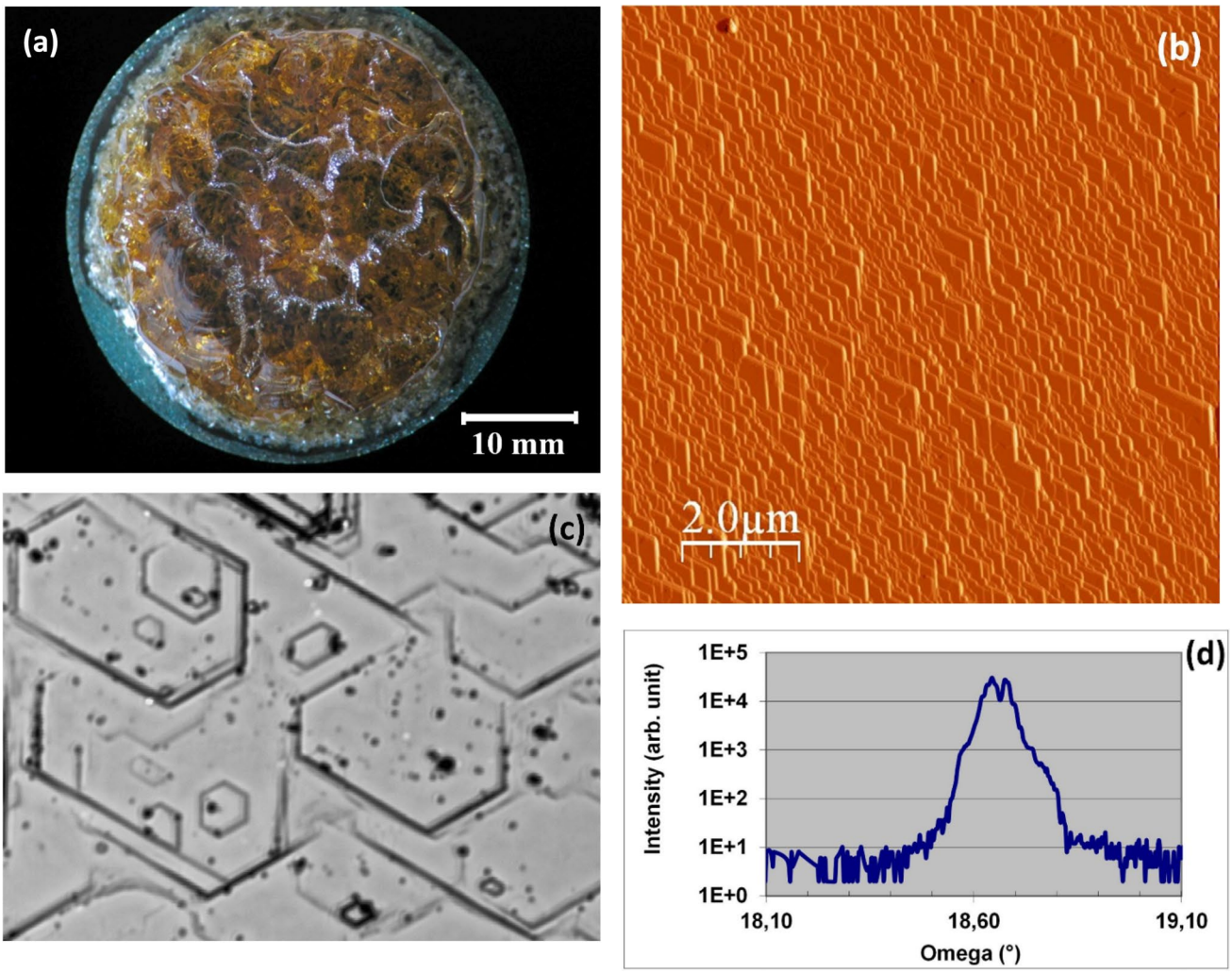

Fig. 4 **a** Photograph of AlN single crystal grown on on-axis SiC showing high density of multi-nucleation; **b** AFM picture showing a step flow growth of AlN on misoriented SiC substrates; **c** laser scanning micrograph (magnification: 20x) of a crystal surface grown on 2° off-oriented SiC; **d** X-ray diffraction rocking curve measured on one of the worst crystals (case study), exhibiting high mosaicity

on the whole surface is via the coalition of these differently nucleated grains, which governs the origin of tilt and/or twist angle between them. This misorientation angle hinders the formation of smooth and perfect (0001) crystallographic plane or otherwise called *c*-plane. But the off-oriented substrate offers closely spaced steps and the growth proceeds with step flow mode as investigated using atomic force microscopy (AFM) and as shown in Fig. 4b. In this case, there are lesser chances for the formation of 3D nuclei. However, after the growth has been completed, the surface of some thicker AlN crystals grown on 2° off-oriented SiC substrates exhibit individual crystallites of different sizes, which looks similar to macro-steps as presented in Fig. 4c. This type of crystallites/features might be formed during cooling down process after the growth, by the recondensation of remaining species still existing in the vapour phase, at temperatures somewhat lower than the actual growth temperature.

In the crystals that consist of 3D nucleated grains, occurrence of low-angle grain boundaries was more probable that increases the mosaicity of the crystal, as seen by XRD measurements. The XRD rocking curve measurements taken on one such a bad crystal (this is the worst crystal grown and only taken for illustration to show a higher mosaicity) grown on on-axis SiC substrate exhibited a rocking curve (peak) with a full width at half maximum (FWHM) value of approximately 0.2° (i.e. 720 arcsec, Fig. 4d). This too high value of FWHM (mosaicity) is unsuitable for device quality substrates and further impedes the usefulness of these crystals for any device applications. Such a high mosaicity is repeatedly reported for AlN crystals grown on SiC substrates [33, 34]. But each single grain is of high quality, and when measured by HRXRD, they show a sharp rocking curve with a FWHM of 70–100 arcsec. It should also be mentioned that all the individual grains are always (0001)-oriented. It is remarkably a good value when compared to the recent literature values of AlN/SiC samples, where the FWHM values of >100 arcsec are reported [35]. This multi-source nucleation could be reduced when off-oriented SiC wafers (between 2° and 4° off) are used as substrates [36] with controlled temperature gradient during growth. In general, the decrease in vapour supersaturation and increase in substrate misorientation angle result in the transformation of a surface with 3D (or 2D) nuclei to that with steps [37]. The off-oriented substrates provide step edges and kink positions for easy attachment of atoms resulting in the step flow growth or layer by layer growth. Further, in PVT growth, higher growth temperatures (> 2000 °C) are beneficial for increasing the surface kinetics (i.e. helping the atoms to properly arrange themselves at the surface). But in AlN/SiC heteroepitaxy, the growth temperature cannot exceed 2000 °C that will result in more thermal etching/evaporation of SiC substrate. Hence, in this case, off-oriented substrates are more beneficial. However, the growth on highly off-oriented substrates ends up with step bunching.

3.5 High etch pit density

Though the lattice constant values favour the selection of hexagonal SiC as a substrate over the other materials, still the small difference in the values between SiC and AlN is good enough to generate stress and misfit edge dislocations at the hetero-epitaxial interface. These edge type dislocations propagate through the crystal length and are detrimental to the lifetime of the devices. But the thick epitaxial layers/bulk crystals, as like in our case, may have the opportunity to offset the lattice mismatch induced stress, with growing thickness due to relaxation, and the quality of the crystal is getting better as the length increases. There were also screw-type dislocations and mixed dislocations found in the crystal, exhibited by wet chemical defect-selective etching. The wet chemical etching allows a first, simple determination of defect structures and density. It was observed that the impurity content of the samples influences the etching time and temperatures of etching. For the etch pit density analyses of the grown AlN samples, the optimum etching condition was found to be 120–150 seconds at 350 °C. Most of the etch pits are hexagonally shaped and are related to threading dislocations. Longer duration of etching resulted in over-etching of the samples and also merging of the etch pits was seen.

Although the middle part of the crystal, depicted in Fig. 2a, looks yellowish in colour, a slice cut from that part exhibits different coloration at the centre (yellow) and at the edges (green). This indicates more impurity incorporation in the perimeter of the crystal. In such cases, high variation in the etch pit density values was observed in the sample. The etch pit density at the yellow regions of such slice is in the order of 10^5 cm^{-2} wherein the dislocations are uniformly distributed (see Fig. 5a). But at the green regions of the same sample, the etch pit density is observed to be at least one order high. The EPD values of different coloured crystals are presented in Table 1. It reveals that the green coloration deteriorates the structural quality of AlN. Carbon and silicon present in the growth environment act as additional sources of local stresses by incorporating into the growing crystal. Some areas, where the macro-holes were formed, the etching was predominant. In Fig. 5b, the orientation of the hole defect is visible, and in this case, the etch pits surrounding the hole defect roughly mirror the shape of this hexagonal hole. Further, the differently oriented lines of the etch pits (for, for example, oriented in the directions [100] and [010] as marked in the figure) meet at 120° angles. As discussed in section 3.1, the hole defect in Fig. 5b reflects the hexagonal symmetry of the crystal and the dislocations in its close proximity are most likely a consequence of stress

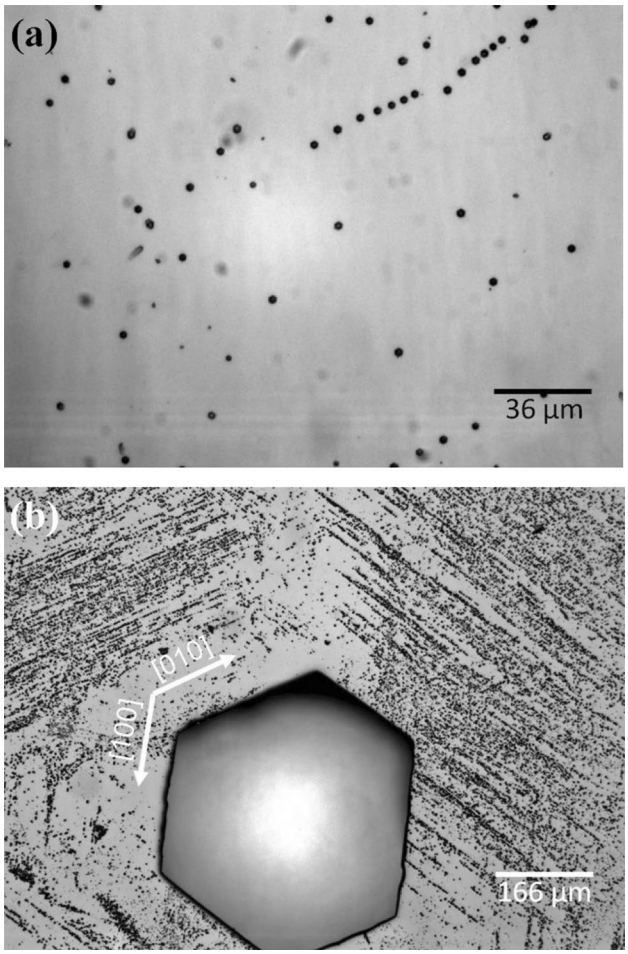

Fig. 5 Optical micrograph of the wet chemically etched surface of the slice cut from the middle part of the crystal of figure-1a, **a** at the centre yellow region with defect density of the order of 10^5 cm^{-2}; **b** at the green-coloured edge where a macro-hole was observed. The etch pits surrounding the macro-hole lie on the lines which mirrors the shape of the hexagonal hole

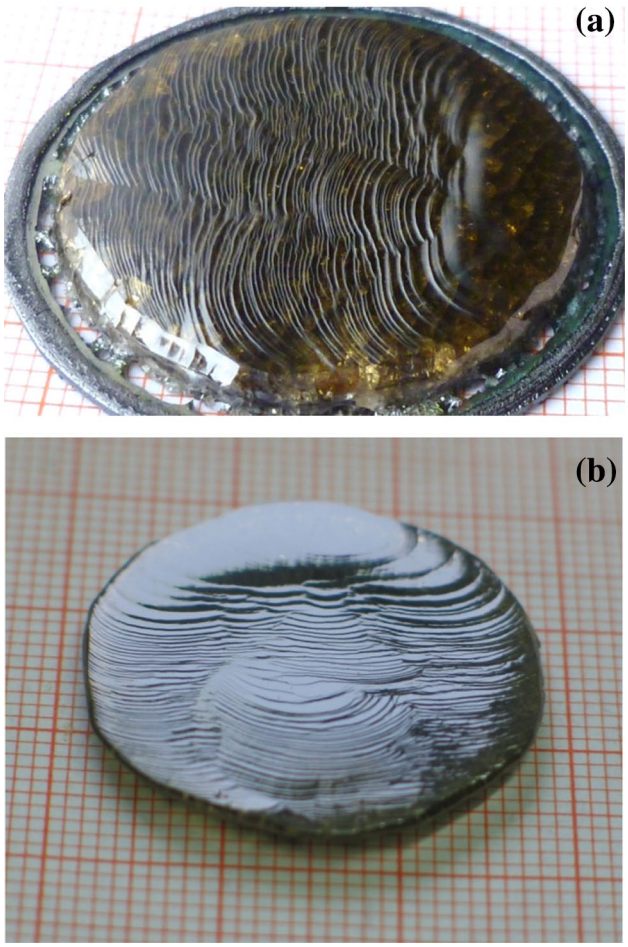

Fig. 6 Photograph of good AlN single crystals grown on off-oriented SiC substrate with optimized process parameters showing **a** highly uniform step flow growth, **b** very smooth surface without any cracks.

deformation traces around the hole and therefore adapt the shape in a macroscopic scale. The lowest etch pit density values of the order of 10^5 cm^{-2} obtained in the good portions of the crystal are bit high for real device applications, as compared to homo-epitaxial grown AlN substrate–10^3 cm^{-2} [6] (for, for example, vertical device structures where the light is extracted through the substrate).

4 Improved crystal growth and properties

With the continuous efforts for the past few years, it was possible to successfully address some of the issues [38, 39]. For example, (i) the growth rate of 50 µm/h from the usual growth rates of 20–30 µm could be achieved by optimizing the growth parameters (especially increasing the temperature gradient, ΔT) in such a way to enhance the mass transport without increasing the decomposition of the SiC substrate (i.e. temperature of growth). Two 1-inch-diameter AlN crystals obtained using the optimized crystal growth conditions, and having improved properties are shown in Fig. 6a and b. Very smooth and uniformly stepped surface morphology could be observed in these crystals. AlN crystals grown in this study (either free-standing wafers or AlN/SiC templates) have better structural properties in comparison with the other reported results of hetero-epitaxial growth [35]. The detailed description of these results could be found elsewhere [36]; (ii) the wafers produced from hetero-epitaxially grown crystals may be used as native seeds for growing high-purity bulk crystals in tungsten crucible set-up with tungsten heating elements (i.e. carbon-free environment), in which these impurities can be reduced to a greater extent, for producing deep UV transparent AlN samples. It is common understanding that the major impurities in bulk AlN crystals are O, C and Si and the key issue is their controllability. Recently, high deep UV transparent AlN crystal grown

under optimized crystal growth conditions was reported [12]. A 60 mm dia. wafer with 98% usable area exhibiting excellent UV transparency in the range 4.43–4.77 eV (260–280 nm) with absorption coefficients of 14–21 cm^{-1} was demonstrated. As long as a reasonable concentration of silicon exists, a high deep UV transparency could be achievable even though relatively high C and O impurities are present in the AlN crystals. Despite the growth issues stated in this article, for the development of large-area native seeds of AlN, hetero-epitaxial growth approach on SiC looks very promising [12, 40] when compared to other approaches, namely self-nucleation and subsequent homo-epitaxial seeding, where the lateral diameter enlargement and iterative growth runs are cumbersome and time-consuming [41]. However, the availability of high-quality large-area (> 4 inch) SiC substrates as seeds with low defect density and with a very few (better zero) micro-pipes is crucial for hetero-epitaxy to grow large diameter AlN single crystals.

5 Persisting issues

5.1 Lower growth rate

Decomposition of the SiC substrate as well as the propagation of micro-pipes can be reduced to some extent, by performing the growth experiments at relatively lower temperatures. However, once when the growth temperature is reduced in the experiment (i.e. lower than 1850 °C), the obtained growth rate is 50 µm/h due to the fact that the growth rate is exponentially decreasing with decreasing temperature. As a result of this, it takes much longer time to grow a fairly thick crystal as compared to homo-epitaxy, in which the growth rate is at least 4 times more. The growth rate is determined mainly by the surface kinetics thus in turn by the crystal growth temperature. The typical temperature of AlN growth on SiC substrates is 200–300 °C lower than that of the growth on native AlN substrates, where high temperatures could be applied, and a growth rate of 200 µm/h could easily be attained. A growth rate of 200–250 µm/h is very attractive and expected for industrial production.

5.2 Unintentional impurities

In AlN, as shown above, the unintentional impurities incorporated during the growth process some way influence the morphology, the chemical content and the coloration of the crystals. However, these impurities do not have much adverse effect on the structural properties. On the other hand, the optical and electrical properties are strongly affected. Particularly for DUV light sources, the optical transparency of the AlN substrate in the wavelength region of 210 – 280 nm is an important requirement for the vertical device structures, where the light extraction through the substrate is necessary. But the unintentional impurities exhibit optical transition bands below the band gap energy, close to blue and UV regions. It is reported that these below-band-gap absorption bands are attributed to the presence of Al vacancies (V_{Al}), substitutional impurities (carbon, oxygen) and their complexes [42]. In addition to the crucible material (mostly TaC) and the purity of the source, the SiC substrate as well determines the extensiveness of the concentration level of these impurities. The origin for a very strong below-band-gap absorption is assigned to the high concentration of C impurities [43] present in the material. While using TaC crucible set-up, unintentional C incorporates markedly from the surrounding graphite environment within the growth chamber and is extremely difficult to completely avoid it. In the PVT growth of bulk AlN single crystals, usually two types of experimental set-ups are widely used: (i) fully tungsten (W)-based set-up, where all the materials for construction such as crucible, substrate holder, heater coils are made of only W, and there is less or no possibility for carbon incorporation from the growth environment; and (ii) TaC-based set-ups, where only the inner crucible and substrate holders are prepared from TaC, and other remaining parts such as heating elements and susceptors are built from graphite. Obviously, there is more carbon incorporation from the surrounding environment during growth. Further the TaC crucible itself consists of a certain level of carbon, which can also add into the growing crystal. In our growth experiments, we have used carburized Ta crucibles kept together with the outer graphite crucible. The details of the growth set-up could be found elsewhere [44]. Optical absorption of crystals grown under different conditions is quite different [13]. From the literature, it is more or less clear that the complete optical transmission up to 210 nm wavelength is a common problem to the AlN crystals grown using all the approaches of PVT growth whether it is self-nucleated, hetero-epitaxially grown or homo-epitaxially grown. Despite the fact that the lowest concentrations of impurities (< 10^{18} cm^{-3}) could be controlled in the pure tungsten set-ups [42], still the below-band-gap optical absorption in the grown crystals is unavoidable. Hence, one may suspect that the native point defects that could be created at very high growth temperatures of AlN might also play a decisive role. The origin and a clear assignment for deep UV optical absorption is still under debate in the literature. It was also reported that the presence of oxygen increases the transparency of the crystals grown under C environment [45]. A certain O-to-C ratio is stated to be required to achieve high deep UV transparency in AlN wafers. In contrast to that conclusion, the superiority of the deep UV transparency was attributed to Si [12], which forms a stable nearest-neighbour C_N–Si_{Al} complex and significantly reduces the absorption and emission peaks. There were already some predictions in the literature

reporting that co-doping AlN crystals with Si suppresses the unwanted 4.7 eV (265 nm) absorption associated with high concentration of isolated carbon acceptors, by forming nearest-neighbour complexes [46]. But, no DUV transparency (> 80%) with homogeneous absorption property in the entire range of 210–280 nm is so far reported for AlN crystals grown along [0001] direction. The hetero-epitaxially grown crystals show even high mosaicity represented by a broader HRXRD FWHM peaks [47] and a high EPD value of 10^5 cm^{-2} revealed by preferential chemical etching. This obstructs the real utilization of AlN as a substrate material for the fabrication of DUV light sources.

6 Conclusions

In the present work, an insight into the common encountered difficulties in growing AlN on SiC substrates by the hetero-epitaxial growth approach by the PVT method has been given. Unlike other approaches and methods, this does not require any additional steps of growing a AlN buffer or patterning on the substrate to reduce dislocations, propagation of micro-pipes defects and also, to avoid cracks due to lattice and thermal expansion coefficient mismatches of substrate material and AlN. Many issues related to this approach, namely micro-hole defect, crystal coloration, crystal cracking, 3D multi-source nucleation, high defect density and low growth rate, have been dealt in detail. Possible suggestions are described for overcoming most of these issues, if not all, like process modification and controlling the initial stages of growth. AlN crystals exhibit different colours such as brown, green, golden yellow or light yellow depending on the growth set-up materials/environments and their corresponding impurity incorporation into the growing crystal. The discussions and results are supported by the various data from different analytical methods. This crystal coloration influences the structural property of the crystal as assessed by wet chemical etching and EPMA. By applying suitable modifications, viz. temperature gradient, controlling the SiC substrate decomposition, a successful growth of bulk AlN single crystals of slightly bigger than 1 inch diameter has been attained using the hetero-epitaxial approach. X-ray rocking curves of the good samples usually show a narrow FWHM value, and the EPDs are also only in the order of 10^5 cm^{-2}. The hetero-epitaxial approach using SiC substrates has an advantage of achieving wide-area AlN substrates (> 4 inch) within a reasonable time frame. Large diameter SiC wafers (about 6 inch) are readily available with relatively moderate cost. As the cost of the SiC wafers may go down further in the next years, this approach would even then be more attractive if the problems like mosaicity, comparatively high defect density are solved. We believe that a possibility of 3–4-inch AlN wafers for device community is imminent in future and further scaling up beyond that size would also be feasible.

Acknowledgments The author wishes to express her thanks to Prof. P. Gille for his encouragements during this research work. The author would also like to gratefully acknowledge the SiCrystal AG for providing good quality SiC substrates. Thanks to Mr. Kai Tandon, a Bachelor degree student, who helped in performing defect analyses. The XPS measurement has been taken with the instrument facility available at Physical Electronics GmbH, Ismaning, and is also being acknowledged here.

Funding Open Access funding enabled and organized by Projekt DEAL. Funding for this study was received from the Bavarian equal opportunity (BGF)

Declarations

Conflicts of interest There are no conflicts to declare

References

1. H. Seppänen, I. Kim, J. Etula, E. Ubyivovk, A. Bouravleuv, H. Lipsanen, Materials **12**, 406 (2019)
2. S. Zhao, Q. Mo, W. Cai, H. Wang, Z. Zang, Photon. Res. **9**, 187 (2021)
3. H. Guan, S. Zhao, H. Wang, D. Yan, M. Wang, Z. Zang, Nano Energy 67, 104279 (2020)
4. C. Himwas, M. den Hertog, F. Donatini, Le Si Dang, L. Rapenne, E. Sarigiannidou, R. Songmuang, E. Monroy, Phys. Status Solidi C 10, 285 (2013)
5. J. Brault, M. Al Khalfioui, M. Leroux, S. Matta, T. Ngo, A. Zaiter, A. Courville, B. Damilano, S. Chenot, J. Duboz, J. Massies, P. Valvin, B. Gil, Proc. SPIE 11686, Gallium Nitride Materials and Devices XVI, 116860T (5 March 2021)
6. D. Li, K. Jiang, X. Sun, C. Guo, Adv. Opt. Photon. **10**, 43 (2018)
7. V. Soukhoveev, O. Kovalenkov, L. Shapovalova, V. Ivantsov, A. Usikov, V. Dmitriev, V. Davydov, A. Smirnov, Phys. Status Solidi C **3**, 1483 (2006)
8. X. Wang, X. Wang, B. Wang, J. Ran, H. Xiao, C. Wang, G. Hu, Front. Optoelectron. China **2**, 113 (2009)
9. J.R. Grandusky, J.A. Smart, M.C. Mendrick, L.J. Schowalter, K.X. Chen, E.F. Schubert, J Crystal Growth **311**, 2864 (2009)
10. J. R. Grandusky, M. C. Mendrick, S. Gibb, J. A. Smart, A. Venkatachalam, S. Graham, L. J. Schowalter, OSA/ CLEO (2011) ATuD3.pdf
11. M. Bickermann, P. Heimann, B.M. Epelbaum, Phys. Status Solidi C **3**, 1902 (2006)

12. Q. Wang, D. Lei, G. He, J. Gong, J. Huang, J. Wu, Phys. Status Solidi A, 1900118 (2019)
13. M. Bickermann, O. Filip, M. Epelbaum. P. Heimann M. Feneberg, B. Neuschl, K. Thonke, E. Wedler, A. Winnacker, Journal of Crystal Growth 339, 13 (2012)
14. R. R. Sumathi, P. Gille, Jpn. J. Appl. Phys. 52, 08JA02 (2013)
15. Kai Tandon, Bacherlor Thesis, Ludwig-Maximilians-University (2009)
16. S.M. Evans, N.C. Giles, L.E. Halliburton, G.A. Slack, S.B. Schujman, L.J. Schowalter, Appl. Phys. Lett. **88**, 062112–1 (2006)
17. T. K. Hossain, J. V. Lindesay, M. G. Spencer, [cond-mat.mtrl-sci].
18. N.B. Singh, A. Berghmans, H. Zhang, T. Wait, R.C. Clarke, J. Zingaro, J.C. Golombeck, J Crystal Growth **250**, 107 (2003)
19. C.G. Moe, Y. Wu, S. Keller, J.S. Speck, S.P. DenBaars, D. Emerson, Phys. Status Solidi A **203**, 1708 (2006)
20. N. Mizuhara, M. Miyanaga, S. Fujiwara, H. Nakahata, T. Kawase, Phys. Status Solidi C **4**, 2244 (2007)
21. W. Hu, L. Guo, Y. Guo, W. Wang, Journal of Crystal Growth 541, 125654 (2020)
22. T. S. Argunova, O. P. Kazarova, M. Yu. Gutkin, E. N. Mokhov, ECS J. Solid State Sci. Technol. 10, 045008 (2021)
23. L. Zhang, H. T. Qi, H. J. Cheng, Y. Z. Shi, Z. P. Lai, M. C. Luo, J. Semicond. 42, 052101 (2021)
24. Y. Zhao, Q. Wang, G. Zhang, J. Huang, D. Fu, J. Wu, Crystal Growth & Design (2021) https://pubs.acs.org/doi/pdf/https://doi.org/10.1021/acs.cgd.0c01511
25. A.K. Gueorguie, D. Nilsson, E. Janzén, Journal of Crystal Growth **338**, 52 (2012)
26. M. Lee, H. Son, H. Lee, J. Moon, H. Kim, J. Park, Z. Liu, M.G. Hahm, M. Yang, U.J. Kim, J. Mater. Chem. C **8**, 14431 (2020)
27. X. Wang, H. Li, J. Wang, L. Xiao, Electron. Mater. Lett. **10**, 1069 (2014)
28. J. Liu, J. Gao, J. Cheng, J. Yang, G. Qiao, Materials Letters **59**, 2374 (2005)
29. S. Mahajan, Appl. Phys. Lett. **80**, 4321 (2002)
30. V. Noveski, R. Schlesser, S. Mahajan, S. Beaudoin, Z. Sitar, MRS Internet J. Nitride Semicond. Res. **9**, 2 (2004)
31. Y.N. Makarov, O.V. Avdeev, I.S. Barash, D.S. Bazarevskiy, T.Y. Chemekova, E.N. Mokhov, S.S. Nagalyuk, A.D. Roenkov, A.S. Segal, Y.A. Vodakov, M.G. Ramm, S. Davis, G. Huminic, H. Helava, J Crystal Growth **310**, 881 (2008)
32. J.H. Harris, R.A. Youngman, R.G. Teller, J Mater. Res. **5**, 1763 (1990)
33. P. Lu, J.H. Edgar, C. Cao, K. Hohn, R. Dalmau, R. Schlesser, Z. Sitar, J Crystal Growth **310**, 2464 (2008)
34. H. Helava, TYu. Chemekova, O.V. Avdeev, E.N. Mokhov, S.S. Nagalyuk, Y.N. Makarov, M.G. Ramm, Phys. Status Solidi C **7**, 2115 (2010)
35. T.S. Argunova, MYu. Gutkin, J.H. Je, A.E. Kalmykov, O.P. Kazarova, E.N. Mokhov, K.N. Mikaelyan, A.V. Myasoedov, L.M. Sorokin, K.D. Shcherbachev, Crystals **7**, 163–1 (2017)
36. R.R. Sumathi, CrystEngComm **15**, 2232 (2013)
37. I. Bryan, Z. Bryan, S. Mita, A. Rice, J. Tweedie, R. Collazo, Z. Sitar, J Crystal Growth **438**, 81 (2016)
38. R.R. Sumathi, R.U. Barz, A.M. Gigler, T. Straubinger, P. Gille, Phys. Status Solidi A. **209**, 415 (2012)
39. E.N. Mokhov, T.S. Argunova, J.H. Je, O.P. Kazarova, K.D. Shcherbachev, CrystEngComm. **19**, 3192 (2017)
40. W. Hu, L. Guo, Y. Guo, W. Wang, of Crystal Growth 541, 125654-1 (2020)
41. G. Wang, L. Zhang, Y. Wang, Y. Shao, C. Chen, G. Liu, Y. Wu, X. Hao, Cryst. Growth Des. **19**, 6736 (2019)
42. M. Bickermann, B.M. Epelbaum, O. Filip, B. Tautz, P. Heimann, A. Winnacker, Phys. Status Solidi C **9**, 449 (2012)
43. R. Collazo, J. Xie, B.E. Gaddy, Z. Bryan, R. Kirste, M. Hoffmann, R. Dalmau, B. Moody, Y. Kumagai, T. Nagashima, Y. Kubota, T. Kinoshita, A. Koukitu, D.L. Irving, Z. Sitar, Appl. Phys. Lett. **100**, 191914–1 (2012)
44. R.R. Sumathi, P. Gille, J Mater Sci: Mater Electron. **25**, 3733 (2014)
45. C. Hartmann, J. Wollweber, A. Dittmar, K. Irmscher, A. Kwasniewski, F. Langhans, T. Neugut, M. Bickermann, Jpn. J. Appl. Phys. 52, 08JA06-1 (2013)
46. B.E. Gaddy, Z. Bryan, I. Bryan, J. Xie, R. Dalmau, B. Moody, Y. Kumagai, T. Nagashima, Y. Kubota, T. Kinoshita, A. Koukitu, R. Kirste, Z. Sitar, R. Collazo, D.L. Irving, Appl. Phys. Lett. **104**, 202106–1 (2014)
47. R.R. Sumathi, Phys. Status Solidi C **11**, 545 (2014)